

**Analogs of the lignan pinoresinol as novel lead compounds for P-glycoprotein (P-gp)
inhibitors**

Jerónimo Laiolo,[†] Tihomir Tomašič,[§] D. Mariano A. Vera,[‡] María L. González,[†] Priscila A. Lanza,[‡], Samanta N. Gancedo,[‡] Žiga Hodnik,[§] Lucija Peterlin Mašič[§], Danijel Kikelj,^{§,*}
María C. Carpinella^{*,†}

[†] *Research Institute of Natural Resources and Sustainability José Sánchez Labrador S.J. (IRNASUS-CONICET), School of Chemistry, Catholic University of Córdoba, Córdoba, Argentina.*

[‡] *Department of Chemistry, QUIAMM – INBIOTEC – CONICET, College of Exact and Natural Sciences, National University of Mar del Plata, Mar del Plata, Argentina.*

[§] *Faculty of Pharmacy, University of Ljubljana, Ljubljana, Republic of Slovenia.*

***Corresponding Author:** María Cecilia Carpinella, Laboratorio de Química Fina y Productos Naturales, Facultad de Ciencias Químicas, Universidad Católica de Córdoba, Avda. Armada Argentina 3555, X5016DHK, Córdoba, Argentina. Tel: 54 351- 4938000, Ext 611. Fax: 54 351-4938061.

EXPERIMENTAL SECTION

General

Compound Database Preparation

The Drugs Now subset of the ZINC database of commercially available compounds was downloaded and the bank of 10.6 million compounds was prepared with OMEGA (OMEGA 3.0.0.1: OpenEye Scientific Software, Santa Fe, NM. <http://www.eyesopen.com>.)¹ to provide an average of 152 conformations per compound.

In addition, a library of PXR ligands^{2,3} was prepared using the same protocol.

3D similarity search of the chemical libraries

In the ligand-based virtual screening for structurally similar compounds to the P-gp inhibitor (\pm)-pinoresinol⁴ in the prepared ZINC Drugs Now subset of compounds and in the library of PXR ligands,^{2,3} 3D similarity searching was implemented in ROCS (ROCS 3.2.2.2: OpenEye Scientific Software, Santa Fe, NM. <http://www.eyesopen.com>)⁵ using (+)-pinoresinol (**1**) as a query. Hits were ranked according to their TanimotoCombo score, which considers molecular shape (shape score) and atom type (color score) similarities.

Docking of identified molecules

The structural model of the P-gp used as receptor of the docking studies was previously proposed in Jara et al.⁶ In that work, this model was subject to stochastic molecular dynamics to obtain average inter-residue distances matching the experimental

distances and challenged to reproduce the right activity order of a pool of known inhibitors, as well as to find binding sites matching those proposed on computational and experimental bases in the literature.^{4,6}

The structures of the putative inhibitors **1-30**, including their possible tautomers and enantiomers where relevant, and of verapamil and tamoxifen were first optimized using the semiempirical PM6 method and further refined at the PBE0/6-31G* levels of theory using the Gaussian09 package⁷. Cyclosporin A (CsA) was left at the PM6 level due to its size.⁷ The nature of minima of the stationary points were checked by the absence of negative eigenvalues of the Hessian. The structures were further translated to the appropriate atom type and Gasteiger charges assigned for preparing the docking protocol using Autodock 4.2.6. The protocol is described in detail in González et al.⁴ Briefly, the protocol involved 2000 runs of Lamarckian genetic algorithm performed for each ligand using Autodock 4.2.6,^{8,9} with 250 individuals and up to 8×10^6 energy evaluations and 10^5 generations and a cluster analysis with a 2.5 Å of root mean square deviation criteria. The VMD 1.8.9 program was used for graphics rendering and analyses.¹⁰

Compounds

PXR ligands **2-9** and **26-34** were prepared as reported previously.^{2,3} All tested compounds were at $\geq 95\%$ purity determined by HPLC.^{2,3}

The structures of the compounds evaluated were characterized by mass and NMR spectroscopy. Spectra are available upon request from the authors.

Biological assays

Equipment and Reagents

3-(4,5-Dimethyl-2-thiazolyl)-2,5-diphenyl-2H-tetrazolium bromide (MTT), rhodamine 123 (Rho 123), cyclosporine A (CsA) and lectin from *Phaseolus vulgaris* (PHA) were obtained from Sigma Aldrich, (Sigma-Aldrich Co., St Louis, MO). Doxorubicin hydrochloride (DOX, 99.8%, Synbias Pharma Ltd.) was obtained from Nanox Release Technology (Buenos Aires, Argentina) and was prepared immediately prior to use dissolved in bi-distilled water. Verapamil hydrochloride 98.0% and tamoxifen citrate (99.7%) were provided by Parafarm (Buenos Aires, Argentina) and were used dissolved in ethanol. RPMI-1640 and Gibco[®] cell culture reagents were purchased from Invitrogen Life Technologies (Carlsbad, CA). Sterile plastic material was purchased from Greiner Bio-One (Frickenhausen, Germany). All solvents were HPLC grade.

FITC mouse anti-human P-glycoprotein was purchased from BD (BD Biosciences, USA). Flow cytometry was performed in a Life Technologies Attune-NxT flow cytometer (Thermo Fisher Scientific, USA).

Cell lines and cell culture

To screen the P-gp modulatory activity of the set of compounds under analysis, the K562 human chronic myelogenous leukemia (CML) cell line and its MDR counterpart, Lucena 1,⁴ were used. Both cell lines were cultured in RPMI-1640 medium supplemented with 10% fetal bovine serum, 2 mM L-glutamine, 100 U mL⁻¹ penicillin and 100 µg/mL streptomycin at 37°C in a humidified atmosphere of 5% CO₂. To maintain drug resistance, DOX at 60 nM was added to the Lucena 1 subline. All experiments were performed after

four days in drug-free medium and with the cells in the logarithmic growth phase. Cell viability above 90% was determined by staining with trypan blue. Lucena 1 cells displayed higher surface P-gp expression (58%) than parental K562 cells (2%), determined by flow cytometry using FITC-conjugated mouse anti-human P-gp antibody. We next examined the degree of resistance of Lucena 1 by determining the concentration of DOX required to inhibit 50% cell proliferation (IC₅₀) using MTT assay.^{11, 12}

Doxorubicin and rhodamine 123 intracellular accumulation assays

The effect of **2-9**, **21**, **23** and **26-34** on DOX intracellular accumulation was investigated. The quantification of the fluorescence inside cells due to the presence of the fluorescent chemotherapeutic drug substrate of P-gp, DOX, is used as a specific way to analyze the inhibition of the efflux of substances mediated by P-gp.

Briefly, 5 x 10⁴ Lucena 1 or K562 cells mL⁻¹ were incubated in duplicate for 1 h, as previously established,⁴ at 37°C with 5% CO₂ in 96-well plates containing complete RPMI-1640 medium, in the presence of 25 µM of each tested compound previously dissolved in DMSO. Following the primary screening, those compounds with promising activity were tested at serial dilutions with the aim of determining their minimum effective concentrations (MEC). Verapamil, tamoxifen and CsA as known P-gp inhibitors, and DMSO at 0.5% v/v (no adverse effects were observed at this concentration) were simultaneously run as positive and negative controls, respectively, while a group of cells with just culture medium was used as the viability control. Following incubation, 5 µM DOX was added and cells were further incubated for 1 h in the dark. Rho 123 is a P-gp fluorescent substrate often employed as an indicator of P-gp activity and thus it was used in

an additional accumulation study for testing the activity of compounds **26** and **27**. The same protocol used for the DOX accumulation assay was performed with this dye, which was added at 500 ng/mL. Subsequently in both assays, cells were placed on ice to stop the reactions and washed twice with cold PBS. Mean fluorescence intensity (MFI) of DOX or Rho 123 retained in 15,000 individual cells was determined by flow cytometry at an excitation wavelength of 488 nm and the emitted light collected with 585/42 nm and 530/30 nm bandpass filters, respectively. Dead cells and cell debris were eliminated by gating the living cells in the forward and side scatter. MFIs were analyzed by Flowjo software (Tree Star, Inc. Ashland, OR). The fluorescence intensity ratio (FIR) was calculated by dividing the MIF of DOX or Rho123 in the presence of the tested compounds by the MIF of DOX or Rho123 alone.

Multidrug resistance reversal assay

The ability of the selected compounds **26** and **27** to sensitize resistant cells to DOX was evaluated in Lucena 1 cells, as well as in parental K562 cells as control, by the MTT colorimetric assay, as previously described.⁴ Briefly, both cell lines at a final concentration of 5×10^4 cells/well were plated in duplicate in 96-well plates with RPMI-1640 medium containing DOX alone (0.27-34 and 1.69-215 μ M for K562 and Lucena 1, respectively) or DOX in combination with 0.39-3.12 μ M of each compound previously dissolved in DMSO. These concentrations were selected since they are equal or similar to the MECs obtained in the DOX accumulation assay. At the highest concentration tested (3.12 μ M) **26** and **27** did not exhibit toxic effects on either cell line (cytotoxicity = 0 and $12.33 \pm 4.26\%$, respectively, in K562 and 0% for both compounds in Lucena 1, Cytotoxicity (%) = $[1 -$

$(\text{Optical density treatment} - \text{Optical density DMSO}) / (\text{Optical density control} - \text{Optical density DMSO})] \times 100$, determined by MTT proliferation assay).¹¹ Negative control wells received only 0.5% DMSO while viability controls contained only supplemented culture medium. Verapamil was used as a positive control. Following 48 h incubation at 37° C with 5% CO₂, 20 µL of MTT (5 mg/mL) solution in sterile PBS was added to each well and plates were incubated for an additional 4 h. Subsequently, the supernatants were removed, and the resulting purple formazan crystals produced from metabolically viable cells were dissolved with 100 µL DMSO. Finally, the absorbance was read at 595 nm in an iMark micro-plate reader (Bio-Rad, USA).

Half inhibitory concentrations (IC₅₀) values were determined as the concentrations of DOX that caused 50% inhibition of cell proliferation (compared to the solvent controls, which showed no differences with respect to viability controls) and were calculated from the mean values of data from wells.

The fold reversal (FR) values for the tested compounds, which indicate the ratio to reduce resistance to DOX, were obtained by calculating the IC₅₀ of DOX alone/ IC₅₀ of DOX in the presence of the tested compounds.^{13,14}

Cytotoxicity on peripheral blood mononuclear cells (PBMC)

To evaluate the effect of **26** and **27** on the proliferation of peripheral blood mononuclear cells (PBMC), an MTT assay was performed as previously described.^{4,11, 15} Fresh heparinized blood was collected from healthy human volunteer donors receiving any treatment. Ethical approval was provided by the Catholic University of Córdoba Research Ethics Board and signed informed consents were obtained from donors. PBMC were

isolated by density gradient centrifugation (Ficoll[®]). Briefly, PBMC at a density of 1×10^5 viable cells/well were treated in duplicate with two-fold serial dilution of both compounds (25-3.12 μ M) previously dissolved in 0.5% DMSO in wells containing RPMI-1640 medium and PHA (10 μ g/mL). After 48 h incubation, MTT was added and the technique proceeded as previously described^{4, 15}. The IC₅₀ values were calculated from the mean percentage of cytotoxicity.

Statistical analysis

The results are expressed as mean \pm SE. Data analysis was carried out with GraphPad Prism software (Graphpad Prism 5.0, Graphpad Software, Inc., CA, USA). The statistical difference in the accumulation of Rho123 or DOX and the potentiation of the cytotoxicity of the latter in the absence and presence of the tested compounds was calculated by the paired Student's *t* test (one-tailed). Comparison of the activity of the compounds with respect to verapamil, tamoxifen and CsA was calculated by one-way analysis of variance (ANOVA) with Bonferroni as post-test. A *p* -value ≤ 0.05 was considered as statistically significant. Each experiment was carried out at least in triplicate.

The IC₅₀ values were calculated from the dose-response curve using GraphPad Prism software analysis responding to at least six concentrations at the 95% confidence level with upper and lower confidence limits.

Supplementary Tables and Figures

Table S1. Brief summary of docking results for PXR ligands and ZINC compounds showing high similarity index with (+)-pinoresinol (1)

Compounds	Estimated free energy of binding (kcal/mol)	Inhibition constant, K_I (nM)
1 (-)	-8.19	987.9
1 (+)	-8.69	428.1
2	-7.45	3460
3	-7.46	3380
4	-7.07	6570
5	-8.22	945.7
6	-8.00	1380
7	-8.38	725.2
8	-8.31	811.0
9	-8.50	591.0
10	-8.01	1350
11	-8.14	1080
12	-7.87	1710
13	-8.95	279.2
14	-9.10	214.7
15	-9.09	216.0

16	-8.78	366.5
17	-9.23	172.9
18	-8.63	475.9
19	-7.89	1633
20 (NH)	-8.59	505.9
20 (OH)	-8.29	803.5
21 (NH)	-8.32	800.8
21 (OH)	-8.56	528.7
22 (NH)	-9.04	237.4
22 (OH)	-9.16	193.0
23 (NH)	-9.23	172.6
23 (OH)	-8.85	325.2
24 (NH)	-8.63	476.0
24 (OH)	-8.92	291.1
25 (OH)	-9.05	242.7
25 (NH)	-8.80	354.3
26	-8.52	566.4
27	-8.66	449.9
28	-8.50	584.1
29	-8.71	413.0
30	-9.12	207.6
tariquidar	-12.36	0.320
verapamil	-9.07	225.5

cyclosporin A	-9.91	54.4
doxorubicin	-8.23	899.7

Table S2. Effect of PXR and selected ZINC compounds on P-gp function in the K562 cell line by doxorubicin accumulation and resistance reversal assays

Compound	Concentration (μM)		
	FIR	FR	
	25	3.12	1.56
2	1.02 ± 0.11		
3	0.74 ± 0.04		
4	1.06 ± 0.03		
5	0.95 ± 0.02		
6	1.00 ± 0.10		
7	0.98 ± 0.01		
8	0.95 ± 0.005		
9	0.92 ± 0.04		
21	0.65 ± 0.32		
23	0.95 ± 0.06		
26	1.04 ± 0.02	1.23 ± 0.08	
27	1.02 ± 0.03	$1.43 \pm 0.06^{**}$	1.12 ± 0.11
28	1.10 ± 0.05		
29	1.07 ± 0.03		
30	1.06 ± 0.02		
31	1.04 ± 0.02		
32	1.01 ± 0.04		

33	1.01 ± 0.03
34	1.02 ± 0.02
Ver	1.03 ± 0.02
Tam	1.04 ± 0.03
CsA	1.10 ± 0.07

Ver: verapamil. Tam: tamoxifen. CsA: cyclosporine A. Fluorescence intensity ratio (FIR); analyses of differences between the intracellular accumulations of DOX in cells treated with the tested compounds compared to control cells were performed by one-tailed paired *t*-test. Fold Reversal (FR) values were calculated as IC₅₀ of DOX alone/IC₅₀ of DOX in the presence of the tested compounds. Statistical comparisons between IC₅₀ of DOX alone or with compound in each treatment were performed by one-tailed paired *t*-test. Results represent the mean ± SE. ****p* < 0.001, ***p* < 0.01 and **p* < 0.05.

Table S3. Effect of 26 and 27 on P-gp function by rhodamine 123 accumulation assay in Lucena 1 cell line

Concentration (μM)	FIR				
	Compound				
	26	27	Ver	Tam	CsA
50	$1.68 \pm 0.15^*$				
25	0.78 ± 0.04	$1.95 \pm 0.10^{**}$	$10.34 \pm 1.62^{**}$	$4.46 \pm 0.34^*$	$11.32 \pm 2.32^{****}$
12.5		$1.43 \pm 0.18^*$	$9.21 \pm 1.38^{***}$	$2.41 \pm 0.20^*$	$10.27 \pm 2.26^{***}$
6.25		1.07 ± 0.05	$8.41 \pm 0.85^*$	$1.39 \pm 0.11^*$	$9.81 \pm 1.72^{***}$
3.12			$7.04 \pm 0.46^*$	0.99 ± 0.10	$9.27 \pm 1.57^{**}$
1.56			$5.27 \pm 0.78^{**}$		$7.08 \pm 1.64^{**}$
0.78			$4.11 \pm 0.53^{**}$		$4.96 \pm 1.41^*$
0.39			$2.71 \pm 0.30^{**}$		$3.18 \pm 0.79^*$
0.19			$1.62 \pm 0.08^*$		$1.80 \pm 0.39^*$
0.098			$1.29 \pm 0.04^*$		1.01 ± 0.07
0.049			1.07 ± 0.07		

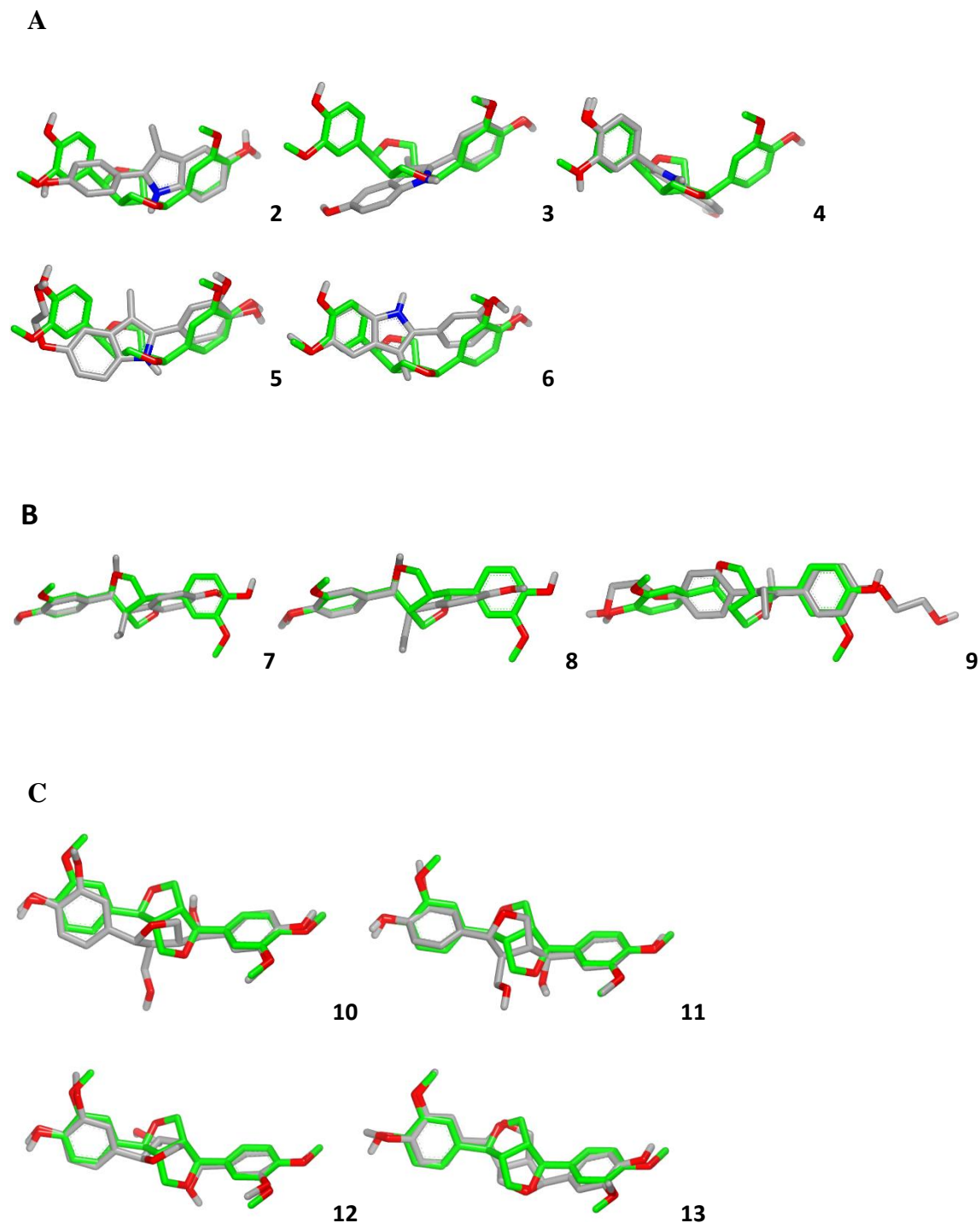
Ver: verapamil. Tam: tamoxifen. CsA: cyclosporine A. Fluorescence Intensity Ratio (FIR); analysis of differences between the intracellular accumulations of Rho123 in cells treated with the tested compounds compared to control cells were performed by one-tailed paired *t*-test. Results represent the mean \pm SE. $^{****}p < 0.001$, $^{**}p < 0.01$ and $^*p < 0.05$.

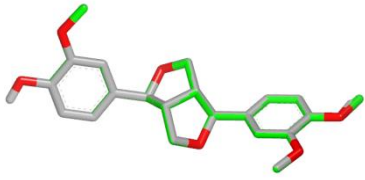
Table S4. Calculated logP values for the assayed compounds

Compounds	ClogP^a
1	1.31
2	3.09
3	2.49
4	3.23
5	2.31
6	4.11
7	4.96
8	6.13
9	4.38
21	2.50
23	2.04
26	5.17
27	5.33
28	6.17
29	6.99
30	7.22
31	2.28
32	3.59
33	4.31
34	4.26

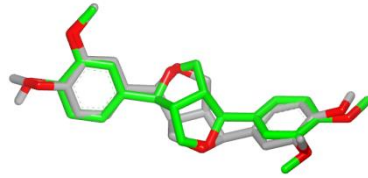
a: calculated using ChemDraw Ultra (BioRad).

Figure S1. (A) Bazedoxifene scaffold-based PXR ligands **2-6**, (B) diethylstilbestrol scaffold-based PXR ligands **7-9** and (C) ZINC compounds **10-25** overlaid with (+)-pinoresinol (**1**) (in green) according to ROCS.

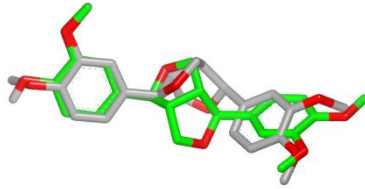




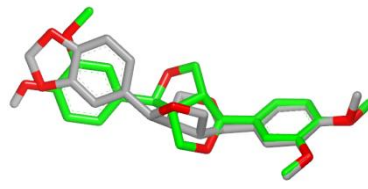
14



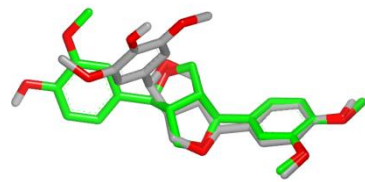
15



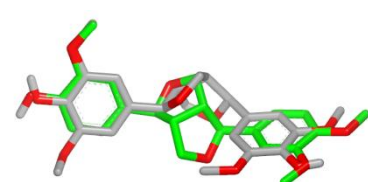
16



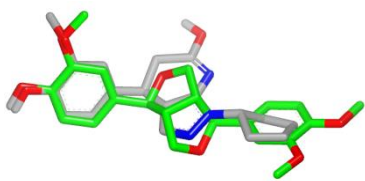
17



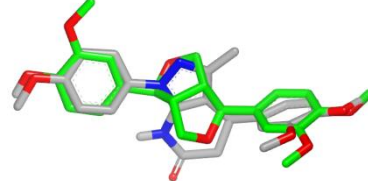
18



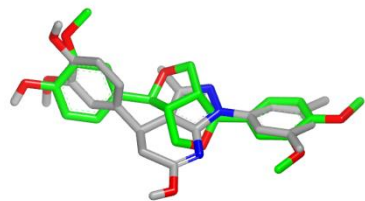
19



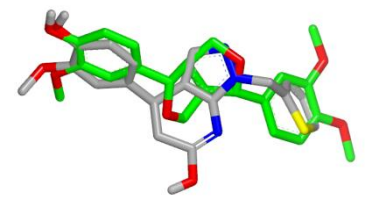
20



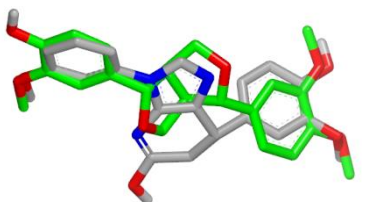
21



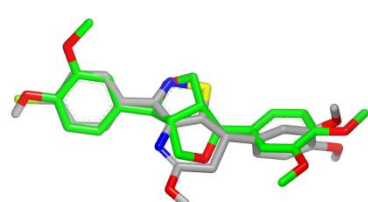
22



23



24



25

Figure S2. Flow cytometric determinations of the effect of compounds **26** and **27** on (A) doxorubicin (DOX) and (B) rhodamine 123 (Rho123) uptake in Lucena 1 cell line. Representative histograms show cells treated with DOX alone in blue, cells treated with DOX and **26** or **27** in red, and cells treated with Rho123 and **26** or **27** in green.

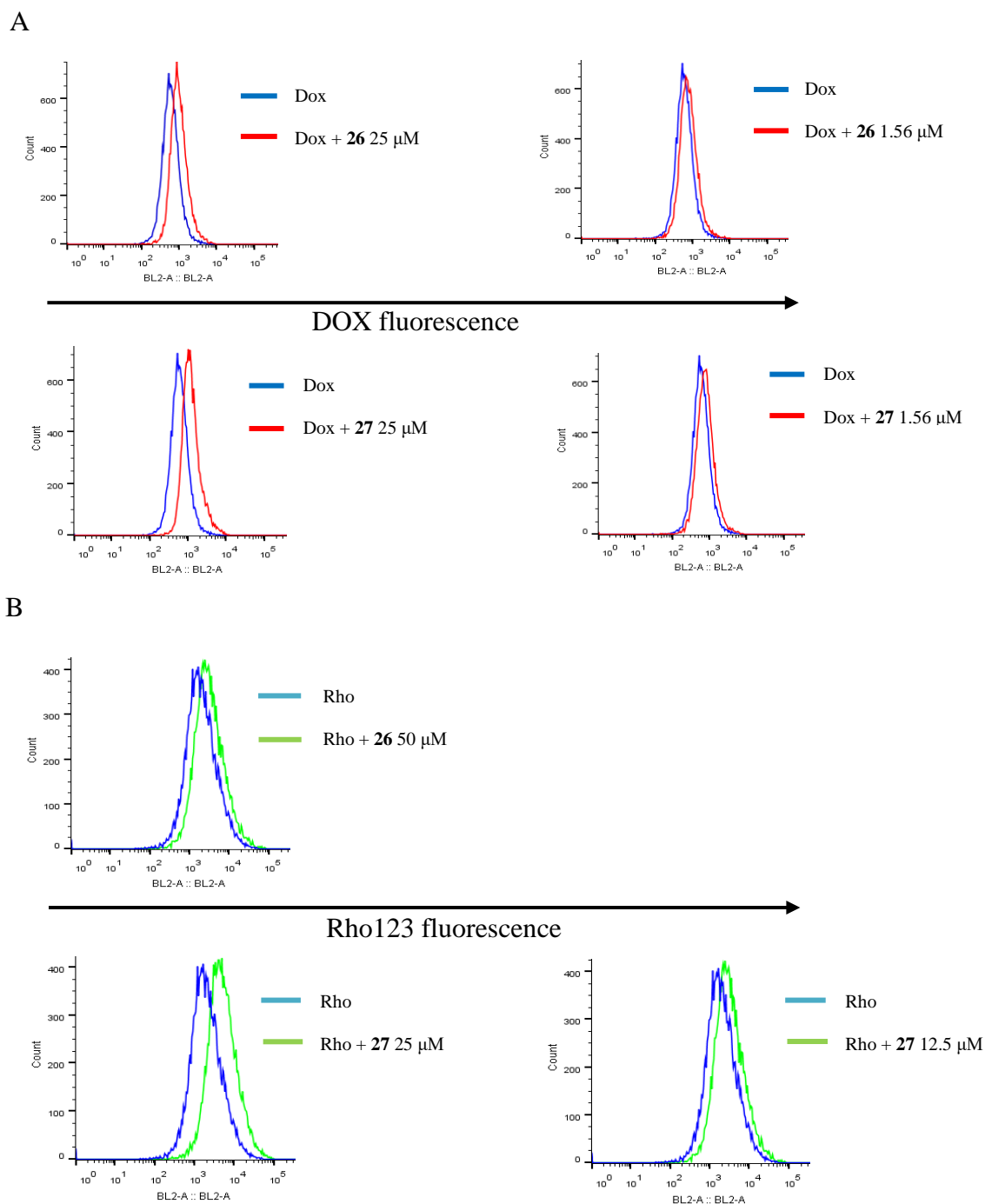


Figure S3. Pose of lowest energy of compound **26** showing its contacts.

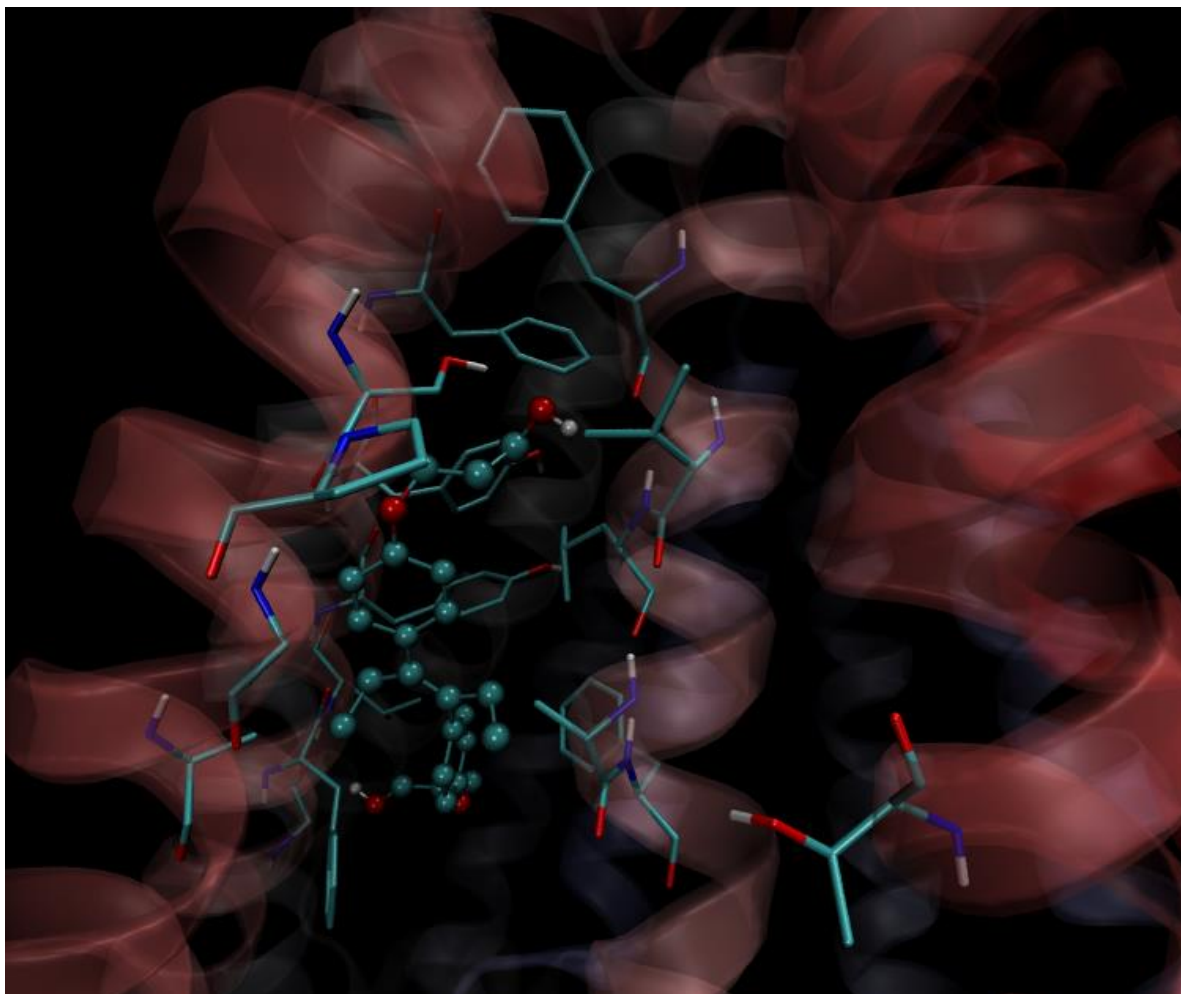


Figure S4. (A) Location of the binding region of compound **27** within the structural model of the human P-gp. (B) Zoom of the site with the surface of the protein colored according to its electrostatic potential (from -0.15 a. u., red, to + 0.15 a. u. blue)

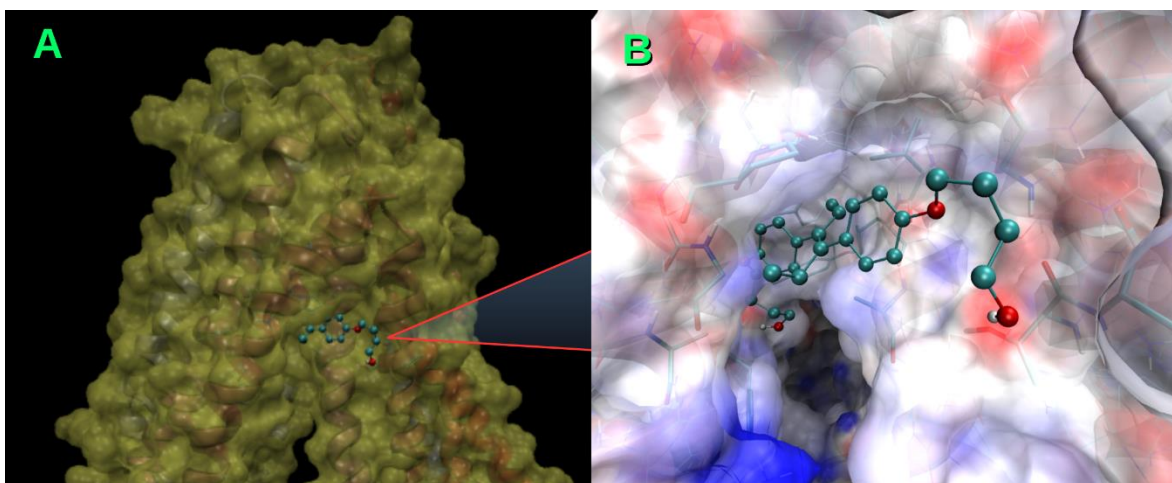


Figure S5. (A) The space occupied by the main sites of doxorubicin (DOX) (-8.23 and -8.16 kcal/mol binding energies) is seen as white translucent surfaces. The protein is shown as cartoon representation with the TMH α -helices colored according to the sequence (from red to blue). The lowest energy poses of compound **27** are superimposed, and colored according to their binding energies, rainbow from -8.66 (red) to -7.44 kcal/mol (violet). (B) Same view rotated -90 degrees around x axis. (C) Same point of view as in B; the structures of **27** are now in magenta and superimposed to the corresponding low energy poses obtained for **26**, all in lime green.

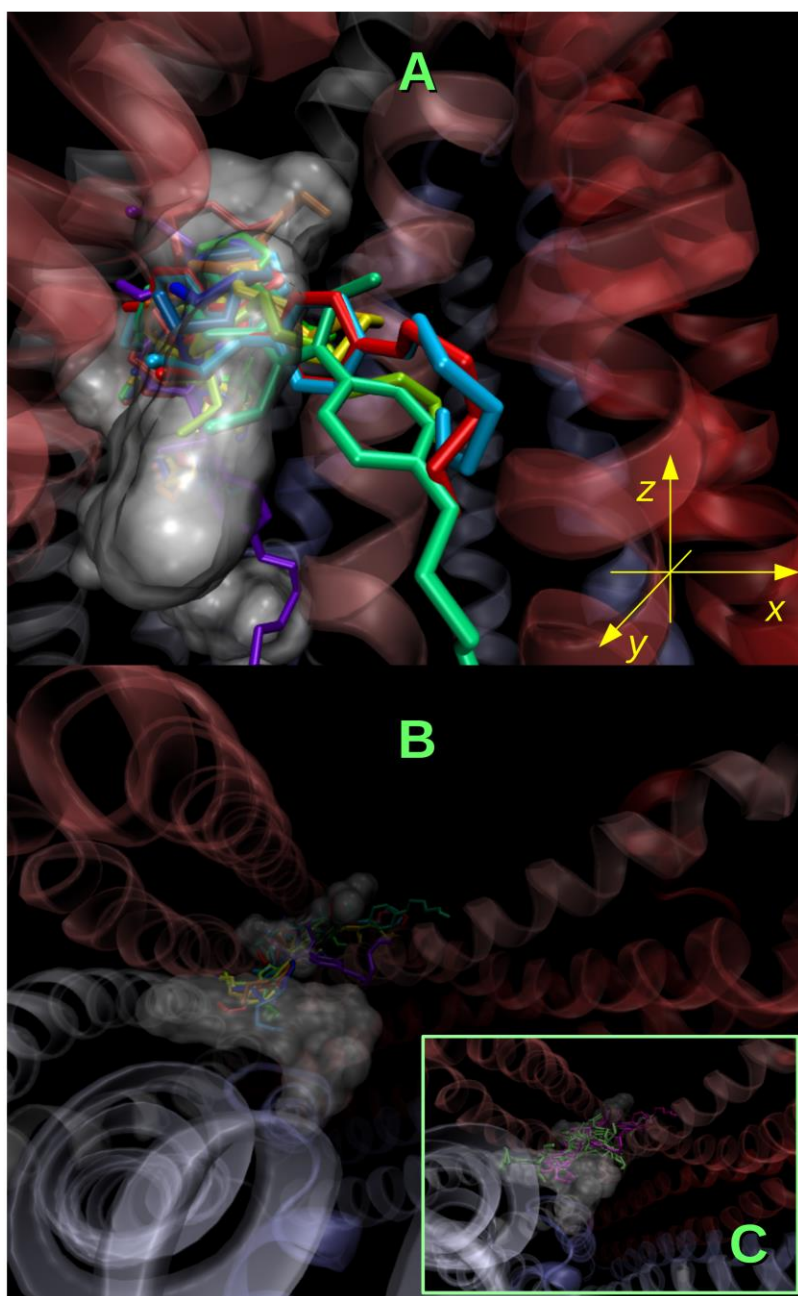


Figure S6. (A) Superimposition of the first lowest energy poses of **27**; colors as in Fig. S5. Main sites of rhodamine 123 (Rho123) appear surrounded by a white wireframe. The poses of **27** overlap only with the secondary Rho123 site, the others being not occluded. (B) View rotated -90 degrees around z axis. (C) View rotated -90 degrees around x axis.

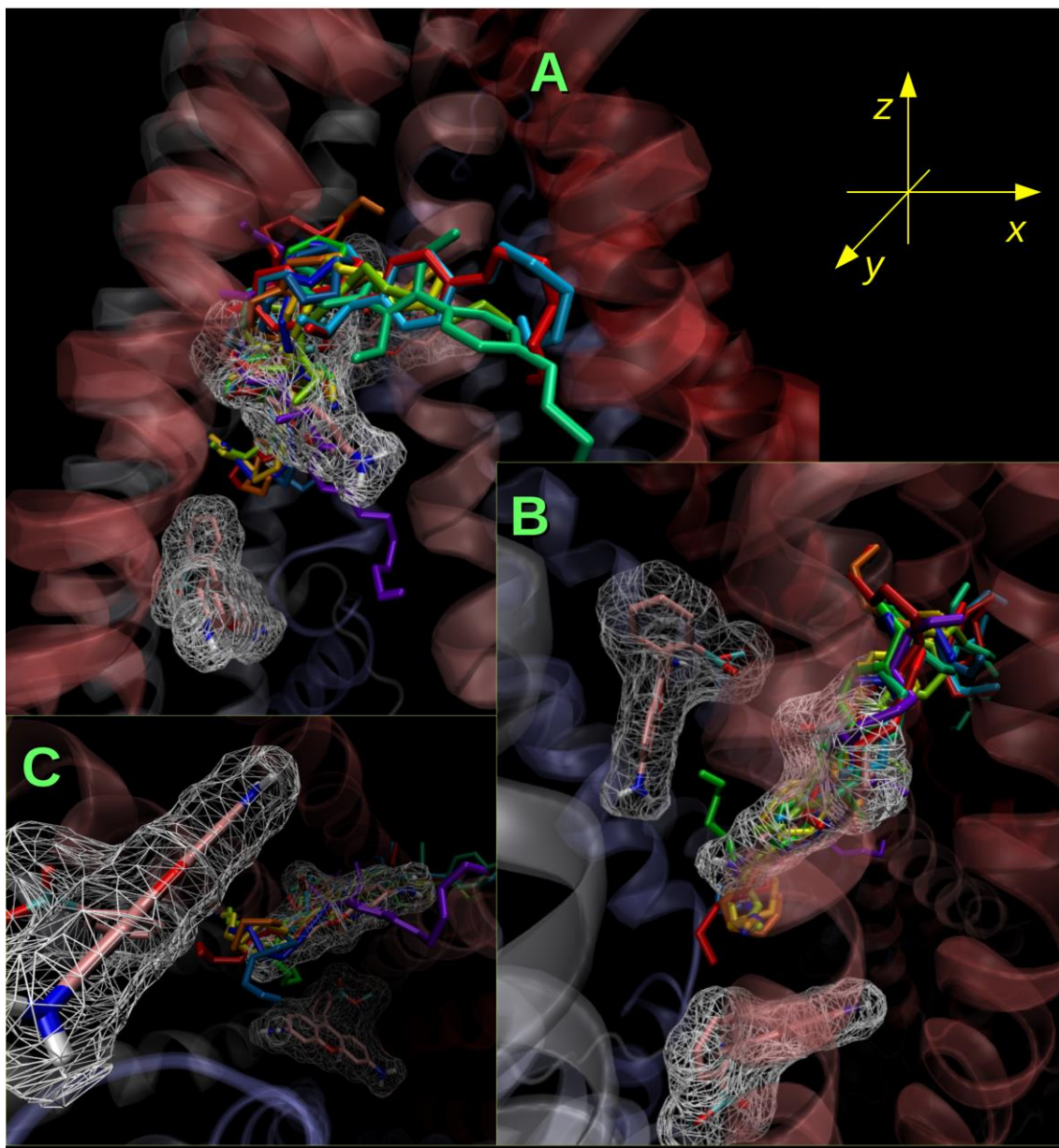


Figure S7. Superimposition of the first lowest energy poses of **26**. Main sites of rhodamine 123 (Rho123) appear surrounded by a white wireframe. Colours and orientation as in previous Fig. S6B.

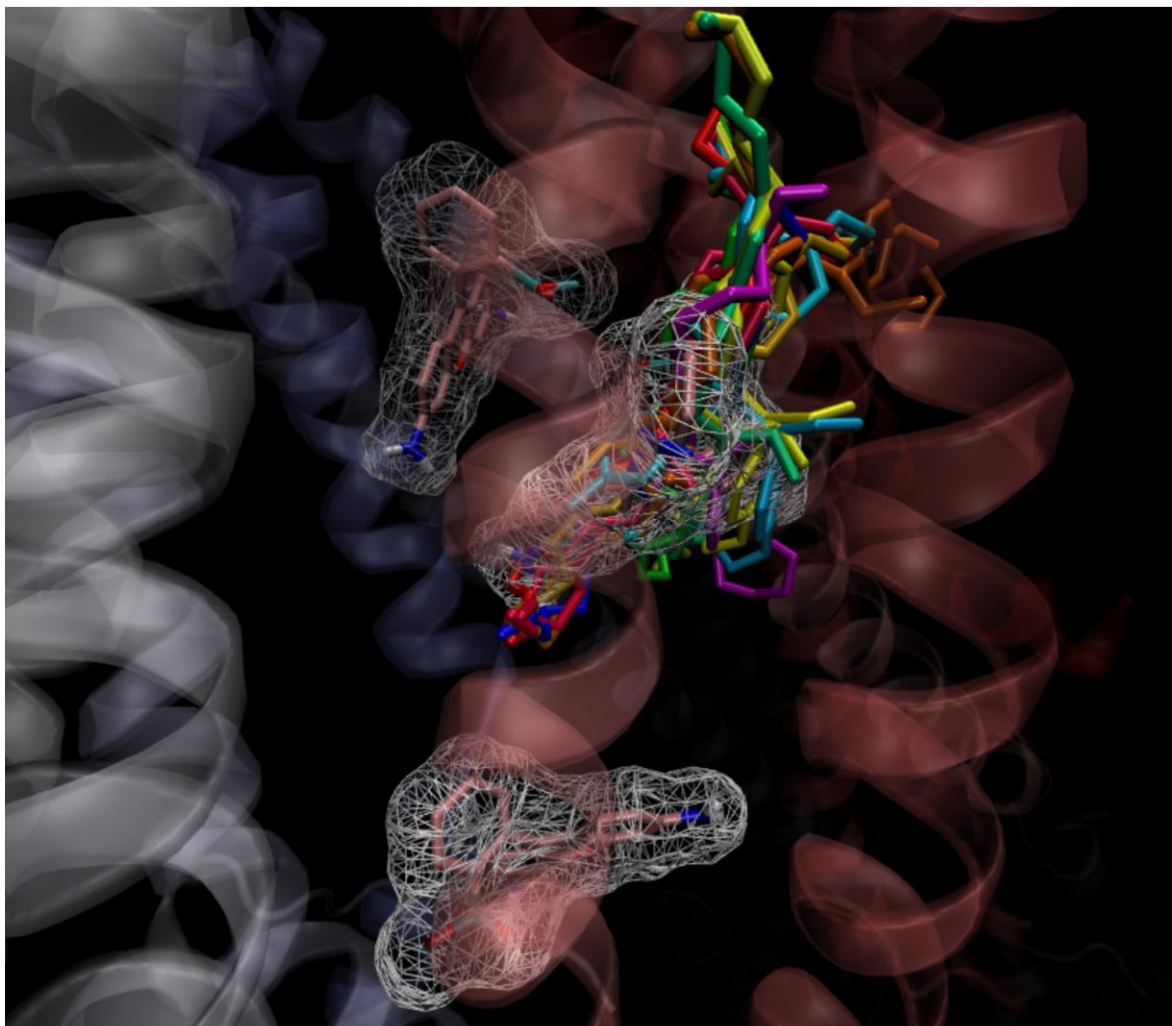


Figure S8. (A) Superimposition of the first poses of cyclosporine A (CsA) (color scheme as in Figs. S5-7 from -9.91 to -9.0 kcal/mol binding energies). The lowest energy pose of CsA overlaps with the three Rho123 binding sites. The other lowest energy poses overlap with at least two of them at once. (B) Rotated -90 degrees around x axis.

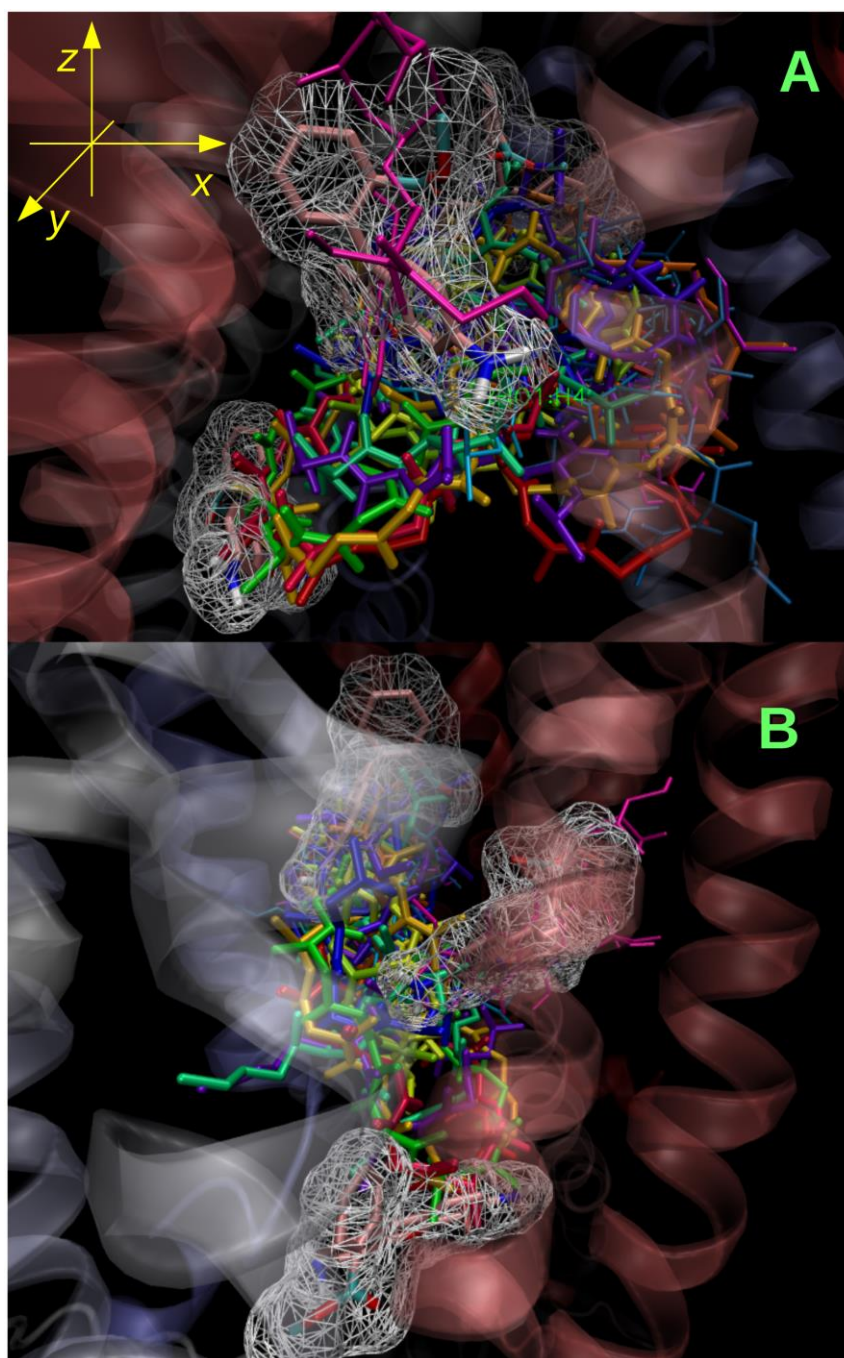
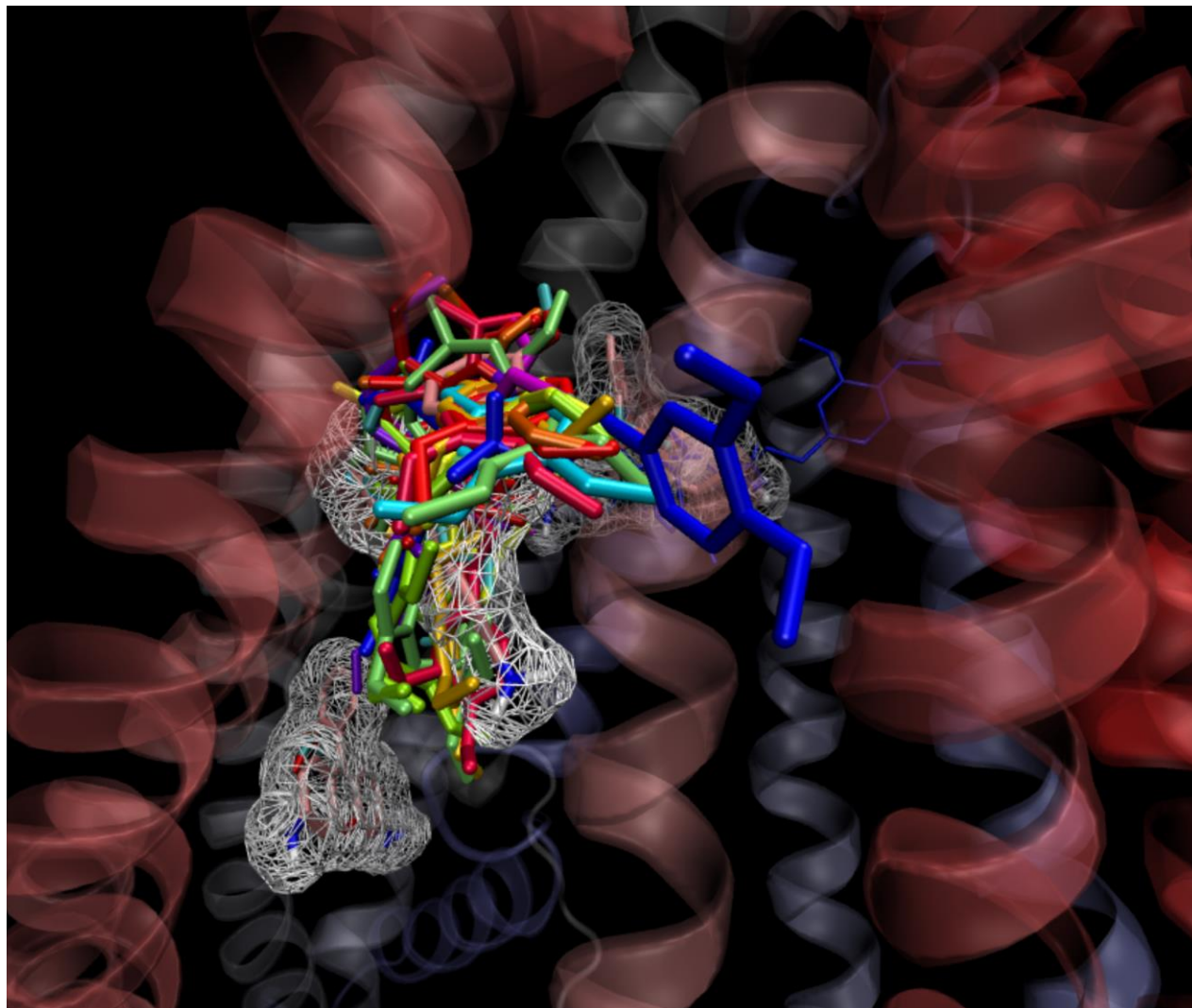


Figure S9. To a lesser extent than CsA, the first lowest energy poses of verapamil overlap with multiple rhodamine 123 (Rho123) sites. Color scheme as Figs. S5-8 above, from -9.07 to 7.97 kcal/mol.



References

- (1) Hawkins, P. C. D.; Skillman, A. G.; Warren, G. L.; Ellingson, B. A.; Stahl, M. T. Conformer Generation with OMEGA: Algorithm and Validation Using High Quality Structures from the Protein Databank and the Cambridge Structural Database. *Journal Chemical Information and Modeling* **2010**, *50*, 572-584.
- (2) Hodnik, Ž.; Peterlin Mašič, L.; Tomašič, T.; Smodiš, D.; D'Amore, C.; Fiorucci, S.; Kikelj, D. Bazedoxifene-Scaffold-Based Mimetics of Solomonsterols A and B as Novel Pregnane X Receptor Antagonists. *J. Med. Chem.* **2014**, *57*, 4819-4833.
- (3) Hodnik, Ž.; Tomašič, T.; Smodiš, D.; D'Amore, C.; Mašič, L. P.; Fiorucci, S.; Kikelj, D. Diethylstilbestrol-scaffold-based pregnane X receptor modulators. *Eur. J. Med. Chem.* **2015**, *103*, 551-562.
- (4) González, M. L.; Vera, D. M. A.; Laiolo, J.; Joray, M. B.; Maccioni, M.; Palacios, S. M.; Molina, G.; Lanza, P. A.; Gancedo, S.; Rumjanek, V.; Carpinella, M. C. Mechanism Underlying the Reversal of Drug Resistance in P-Glycoprotein-Expressing Leukemia Cells by Pinorexinol and the Study of a Derivative. *Front. Pharmacol.* **2017**, *8*.
- (5) Hawkins, P. C. D.; Skillman, A. G.; Nicholls, A. Comparison of Shape-Matching and Docking as Virtual Screening Tools. *J. Med. Chem.* **2007**, *50*, 74-82.
- (6) Jara, G. E.; Vera, D. M. A.; Pierini, A. B. Binding of modulators to mouse and human multidrug resistance P-glycoprotein. A computational study. *J. Mol. Graph. Modeling* **2013**, *46*, 10-21.
- (7) Frisch, M. J.; Trucks, G. W.; Schlegel, H. B.; Scuseria, G. E.; Robb, M. A.; Cheeseman, J. R.; Scalmani, G.; Barone, V.; Mennucci, B.; Petersson, G. A.; Nakatsuji, H.; Caricato, M.; Li, X.; Hratchian, H. P.; Izmaylov, A. F.; Bloino, J.; Zheng, G.; Sonnenberg, J. L.; Hada, M.; Ehara, M.; Toyota, K.; Fukuda, R.; Hasegawa, J.; Ishida, M.; Nakajima, T.; Honda, Y.; Kitao, O.; Nakai, H.; Vreven, T.; Montgomery, J., J. A.; Peralta, J. E.; Ogliaro, F.; Bearpark, M.; Heyd, J. J.; Brothers, E.; Kudin, K. N.; Staroverov, V. N.; Kobayashi, R.; Normand, J.; Raghavachari, K.; Rendell, A.; Burant, J. C.; Iyengar, S. S.; Tomasi, J.; Cossi, M.; Rega, N.; Millam, J. M.; Klene, M.; Knox, J. E.; Cross, J. B.; Bakken, V.; Adamo, C.; Jaramillo, J.; Gomperts, R.; Stratmann, R. E.; Yazyev, O.; Austin, A. J.; Cammi, R.; Pomelli, C.; Ochterski, J. W.; Martin, R. L.; Morokuma, K.; Zakrzewski, V. G.; Voth, G. A.; Salvador, P.; Dannenberg, J. J.; Dapprich, S.; Daniels, A. D.; Farkas, O.; Foresman, J. B.; Ortiz, J. V.; Cioslowski, J.; Fox, D. J. Gaussian 09, Revision A.01. *Gaussian, Inc., Wallingford CT* **2009**.
- (8) Morris, G. M.; Goodsell, D. S.; Halliday, R. S.; Huey, R.; Hart, W. E.; Belew, R. K.; Olson, A. J. Automated docking using a Lamarckian genetic algorithm and an empirical binding free energy function. *J Comput Chem* **1998**, *19*, 1639-1662.
- (9) Morris, G. M.; Huey, R.; Lindstrom, W.; Sanner, M. F.; Belew, R. K.; Goodsell, D. S.; Olson, A. J. AutoDock4 and AutoDockTools4: Automated docking with selective receptor flexibility. *J Comput Chem* **2009**, *16*, 2785-2791.
- (10) Humphrey, W.; Dalke, A.; Schulten, K. VMD: Visual molecular dynamics. *J. Mol. Graph.* **1996**, *14*, 33-38.
- (11) Joray, M. B.; Trucco, L. D.; González, M. L.; Diaz Napal, G. N.; Palacios, S. M.; Bocco, J. L.; Carpinella, M. C. Antibacterial and Cytotoxic Activity of Compounds Isolated from *Flourensia oolepis*. *Evid. Based Complement. Alternat. Med.* **2015**, *2015*, 11.

- (12) Joray, M. B.; Villafañez, F.; González, M. L.; Crespo, M. I.; Laiolo, J.; Palacios, S. M.; Bocco, J. L.; Soria, G.; Carpinella, M. C. P53 tumor suppressor is required for efficient execution of the death program following treatment with a cytotoxic limonoid obtained from *Melia azedarach*. *Food Chem. Toxicol.* **2017**.
- (13) Xu, X.; Zhang, Y.; Li, W.; Miao, H.; Zhang, H.; Zhou, Y.; Li, Z.; You, Q.; Zhao, L.; Guo, Q. Wogonin reverses multi-drug resistance of human myelogenous leukemia K562/A02 cells via downregulation of MRP1 expression by inhibiting Nrf2/ARE signaling pathway. *Biochem. Pharmacol.* **2014**, 92, 220-234.
- (14) Huang, M.; Jin, J.; Sun, H.; Liu, G. Reversal of P-glycoprotein-mediated multidrug resistance of cancer cells by five schizandrins isolated from the Chinese herb *Fructus Schizandrae*. *Cancer Chemother. Pharmacol.* **2008**, 62, 1015-1026.
- (15) González, M. L.; Joray, M. B.; Laiolo, J.; Crespo, M. I.; Palacios, S. M.; Ruiz, G. M.; Carpinella, M. C. Cytotoxic Activity of Extracts from Plants of Central Argentina on Sensitive and Multidrug-Resistant Leukemia Cells: Isolation of an Active Principle from *Gaillardia megapotamica*. *Evid. Based Complement. Alternat. Med.* **2018**, 2018.